18TH WORLD CONFERENCE ON EARTHQUAKE ENGINEERING
WCEE2024
MILAN

MILAN, ITALY
30TH JUNE - 5TH JULY 2024
www.wcee2024.it

EUROPEAN MACROSEISMIC SCALE 1998 (EMS-98) APPLICATION TO THE TARGET REGION OF SERAMAR PROJECT MIRRORING THE 2023 EARTHQUAKE SEQUENCE

L. Abrahamczyk[1], J. Schwarz[2], M.C. Genes[3], P. Gülkan[4], T. Langhammer[2], Ch. Kaufmann[2]

[1] Chair of Advanced Structures, Faculty of Civil Engineering, Bauhaus-University Weimar, Germany, lars.abrahamczyk@uni-weimar.de

[2] Earthquake Damage Analysis Center, Faculty of Civil Engineering, Bauhaus-University Weimar, Germany

[3] Eastern Mediterranean University, Civil Engineering Department, Famagusta, Cyprus

[4] Bashkent University, Ankara, Türkiye

Abstract: *The description of building vulnerability and reliable damage prognoses for different impact levels are the key elements for seismic risk studies, especially in the case of the assessment of a whole building stock. Within the different phases of the Turkish–German joint research project on Seismic Risk Assessment and Mitigation in the Antakya–Maras, Region – SERAMAR, the region's specific earthquake hazard and fault situation were assessed; the vulnerability of the building stock was assigned by street view inspection based on European Macroseismic Scale 1998 (EMS-98). Assigned vulnerability classes recognize structural particularities and design defects within optimistic, pessimistic and most likely scenarios. In addition, the social vulnerability and resilience to earthquake disasters have been studied and could be overlapped to the damage prognosis as the major outcome of intensity based scenarios assuming the epicenter close to the city center or along existing fault lines. The ancient city of Antakya, also known as the historic Antioch on the Orontes, lies in the southernmost tip of Turkey, and its development has extended over an alluvial plain through which the river Asi flows. The building damage and casualties of several different intensities of earthquake scenarios had been estimated for the purpose of qualified planning decisions by regional authorities. Judging from historical precedence, major earthquakes on the branch of the Dead Sea–East Anatolian fault system have a real potential for occurrence in the city. The devastating February 2023 Kahramanmaras earthquake sequence affecting Turkey and Syria caused tremendous damage within the Antakya region and especially to the target region of SERAMAR project where a detailed survey of the building stock has been performed. For the first time, such a unique database and the previously derived scenarios can be validated. The paper mirrors the results of the SERAMAR project in the light of the shaking effects of the February 2023 earthquake sequence. Aspects like assignment of EMS-Intensity in case of cascading events, the adoption of shake maps calibrated to the observation and the reliability of risk studies will be addressed. Focusing on previously instrumented and numerically investigated buildings, representative RC and masonry types are considered enabling the comparison to existing fragility functions. On this basis, the differences between empirical and analytical damage prognosis are discussed.*

1. The SERAMAR Project

The Turkish-German joint research project on Seismic Risk Assessment and Mitigation in the Antakya-Maras-Region – SERAMAR was initiated and conducted in close collaboration with local partners and the Earthquake Damage Analysis Center (EDAC) at Bauhaus-Universität Weimar (Abrahamczyk et al. 2013). Within the project, a complete building stock survey was carried out (despite the fact of the high effort), because any systematic elaboration of a building typology for risk assessment starts and fails with the level and quality of the building survey. Further, tools for earthquake risk mitigation combined with engineering seismology and social science were utilized within an environment where research entities from the European research area, local universities in Turkey, professional associations, and local governments were able to establish a unique partnership. The study was additionally motivated by the rapid expansion of the urban settlements with many vulnerable buildings added to its stock in Turkey during the last several decades.

Figure 1. Sample pictures of Antakya's building stock and recent damages (© EDAC & M.C. Genes).

The ancient city of Antakya lies in the southernmost tip of Turkey, and is built on an alluvial plain through which the river Asi flows. The city, founded in 300 BC, has been an important confluence of states, faiths and peoples from its earliest times. Within the different project phases the region's specific earthquake hazard, the vulnerability of the city's building stock based on the EMS-98 principles (Grünthal et al. 1998), and the social vulnerability and societal vigorousness to earthquake disasters at different levels of society are identified and elaborated (see also http://seramar.edac.biz).

2. SHAKEmaps of February 2023 Kahramanmaras earthquake sequence

The seismic event that occurred in the Turkey-Syria region on February 6, 2023 (USGS 2023), holds a distinctive characteristic whereby multiple fault ruptures were involved. The event had an intensity of XI on the Modified Mercalli Intensity Scale and EMS-98. Initially, an earthquake with a magnitude of M 7.8 occurred in Kahramanmaras, which was subsequently followed by the rupture of a separate fault 9 hours later, resulting in a consecutive earthquake of magnitude M 7.5 in the area. Considering the cumulative effects of these cascading events is crucial for assessing damage prognosis and overall hazard, as multiple earthquakes can amplify the damage caused by subsequent events.

The sequenced event led to the collapse of 6'500 buildings and more than a million buildings suffered damages of different levels, causing the death of 42'310 people according to different reports (AFAD 2023), with a total of 7'184 recorded aftershocks. Ground motion records from 260 seismic stations were made available for the M7.8 event through the main earthquake monitoring networks currently operating in Turkey (Hancilar et al. 2023). The macroseismic dataset is collected in terms of felt reports through internet-based questionnaires from the USGS "Did you feel it?" (DYFI) (Wald et al. 1999) database, a total of 2'014 reports are collected which are clustered into 420 data points.

The hazard level in terms of SHAKEmap resulting from the M7.8 event is illustrated in Figures 2. The initial SHAKEmap underwent a series of updates over time, with a total of 16 different versions calculated (as of 1st May 2023), the final version being generated 46 days post-event. Due to the complex nature of the event's rupture, adjustments to the rupture dimensions were updated several times, introducing an added layer of uncertainty into the final SHAKEmap results. The ultimate rupture dimensions were incorporated into (version 7) approximately 4 days following the event, alongside the integration of data from available seismic recording stations (Hasan et al. 2023).

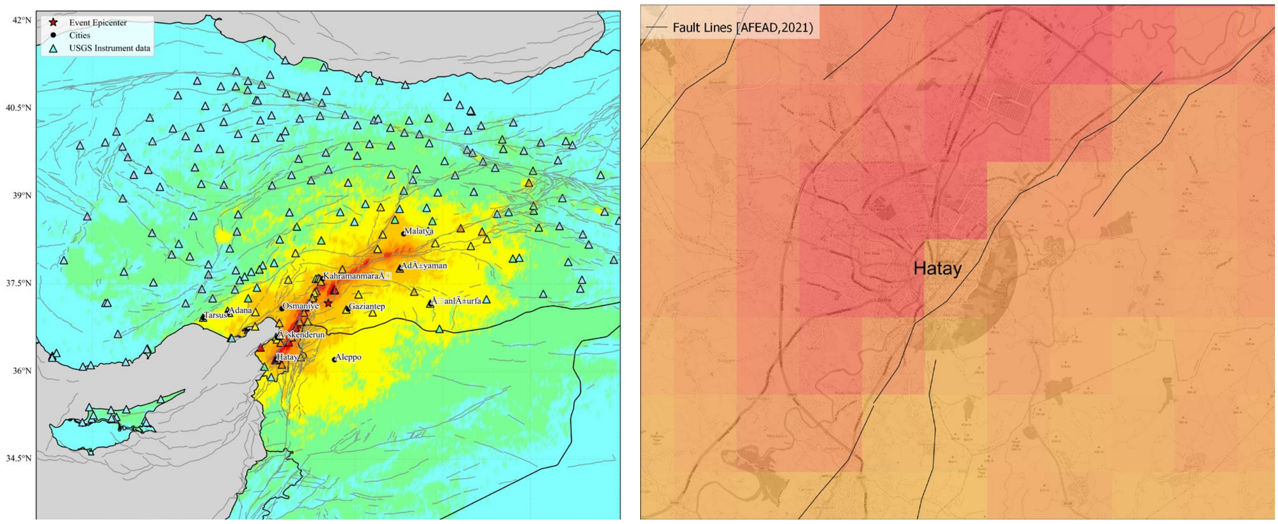

MMI	< I	II	III	IV	V	VI	VII	VIII	IX	X
PGA [%g]	0.046	0.297		2.76	6.2	11.5	21.5	40.1	74.7	>139

Figure 2. SHAKEmaps calculated for cascading events during the 2023 Kahramanmaras, Turkey-Syria sequenced earthquake.

3. Building stock survey

3.1. Application of EMS-98 building typology

Basic building Types

In general, statistical data being relevant for an engineering evaluation of the building's vulnerability were not available at the time the project was started. A first building typology was derived on the basis of data collected during the building stock survey in 2005 and its completion in 2009 (Abrahamczyk et al., 2013). In 2012, a further field survey was conducted to particularly investigate masonry buildings (Erberik et al., 2013). Nowadays, housing census and building permits should be available; they can be used for an up-dated regional risk analysis. All data were mapped (see Figure 4) using a GIS-tool together with the elaborated hazard parameters and risk data layers (i.e., subsoil conditions, topography). As a result, buildings of different material types representative for the various times could be found as well as buildings consisting of several materials. Especially in the suburb areas, oftentimes the ground floor is constructed with a different material than the upper floors due to different construction periods. Typically, adjacent buildings are attached to each other because of limited space and without following any rules. Within the building stock survey following parameters were gathered:

- Material of the structural system,
- Number of stories,
- Peculiarities of the structural system (vulnerability affecting solutions like soft story, cantilevering upper story, widely/ rampant built) see Figure 3,
- Peculiarities of the location (typographical situation like top of a steep slope),
- Utilization (residential, commercial, etc.).

a) RC: Soft/open first story

b) rampantly built

c) Masonry buildings with irregularities in elevation

d) Clusters of masonry buildings

Figure 3. Examples of observed vulnerability affecting construction characteristics ("defects").

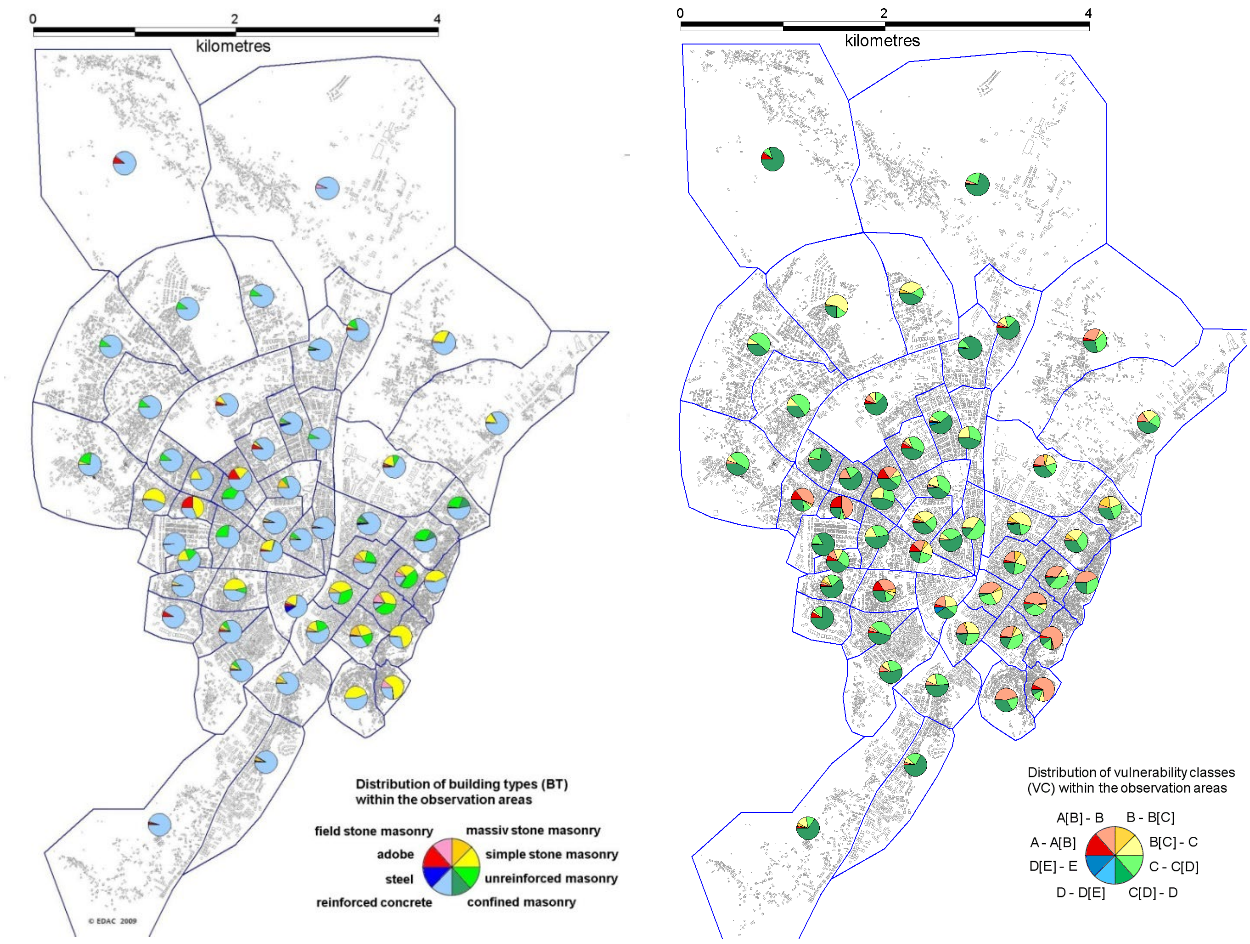

Figure 4. Distribution of: left: building types (primary classes); right: vulnerability classes in Antakya on the basis of detailed building stock survey.

3.2. EMS-98 vulnerability assignment

Based on the elaborated survey data and the application of the EMS-98 the existing building stock was classified and the vulnerability classes for each building determined / assigned (see Figure 4; Schwarz et al. 2008; Schwarz 2010 & 2011; Abrahamczyk et al. 2014). The EMS-98 explicitly allows the assignment of transition classes and the consideration of vulnerability affecting factors (regularity, workmanship, state of maintenance). It is one of the inherent advantages of the EMS-98 that the ranges of the vulnerability can be used to indicate the scatter of existing realizations and – with rather simplified graphical elements – the probability of expectation. For each vulnerability class, a description of the probable quality (damage grades) and extent (quantity of their occurrence) in dependence on the level of shaking is given (Schwarz et al., 2021).

Advantage of the comprehensive survey was taken for a refinement of the intensity-based scenarios by:

- composition of vulnerability classes for each building type (e.g., MM-massive stone, MS-simple stone, RC-reinforced concrete frames, etc.);
- definition of an average vulnerability class for each building type (as well as upper and lower-bound variations);
- distinction of building types by consideration of their layout irregularity, as well as structural peculiarities.

To indicate the appropriateness of a refined vulnerability assignment to the building stock, different approaches were considered and three different cases conducted:

a. Strict assignment of the *most likely vulnerability* (MLV) class according to EMS-98 neglecting any consideration of further vulnerability affecting parameters. Transition classes are not used. Vulnerability class C is assigned to all reinforced concrete buildings, which means ignoring the positive effect of earthquake-resistant design. This could actually be expected due to the high seismic risk indicated by the highest seismic zone and the valid seismic provisions. At least in theory, buildings older than 60 years can be assumed to be without seismic provisions (VC C).

b. Use of the *engineer-assigned vulnerability* (EAV) class assigned on the basis of all collected data related to the building stock. Transition classes are explicitly used. Vulnerability class CD is used as basis for all RC buildings and is modified (mostly reduced) by the vulnerability affecting design aspects (like soft stories). This assumption considers the expected earthquake-resistant design (ERD) in high seismic areas, which is actually implicit in the assignment of vulnerability class D. Also, the experience of the behavior of RC buildings during the recent devastating earthquakes in Turkey support the assumption of a relatively high vulnerability and the acceptance of a pessimistic damage prognosis.
c. Allocation of a *pessimistic vulnerability* (PV) class to the entire building stock by decreasing the engineer-assigned vulnerability class by one class. This will consider the uncertainties, which could not be investigated in the frame of the building stock survey, such as:
    - Material properties: Low quality (e.g., concrete strength) due to the ingredients used
    - Frame discontinuities: Typical for Turkey, evident only by detailed investigation
    - Short/ long dimension ratios and workmanship.

3.3. Fragility functions

Pre-selection for the dominant building types

In parallel to the empirical-based risk assessment different analytical risk scenarios on the basis of fragility functions from different authors were applied to check the quality and reliability of the risk scenarios (Schwarz et al. 2015; Abrahamczyk et al. 2014). Figure 5 shows examples of available fragility functions for (a) five-story (SC 2) Reinforced Concrete (RC) frame structures with masonry infill walls and (b) two-story brick masonry structures compared for the limit state of collapse by the use of the “Fragility Function Manager” (Silva et al., 2011). The comparison of the fragility functions indicates a large scatter for masonry and reinforced concrete buildings. The partially contradicting tendencies (optimistic, pessimistic) within the curves support the demand (and the SERAMAR inherent project concept) to put the local building stock under a complex evaluation and detailed investigation procedure.

The comparison of the proposed (not always applicable) fragility functions indicates the need of an adjustment to the existing building stock to come up with reliable damage scenarios. It also shows that the quality of any analytical damage scenario will be mainly influenced by the selection of the fragility functions and adaption of the fragility functions to the local building typology. For the risk assessment of a building stock different aspects are of importance: the validity of the fragility functions; the number of subtypes, and the reduction of the uncertainty of the action/impact influencing parameters (e.g., soil characteristic’s, topography).

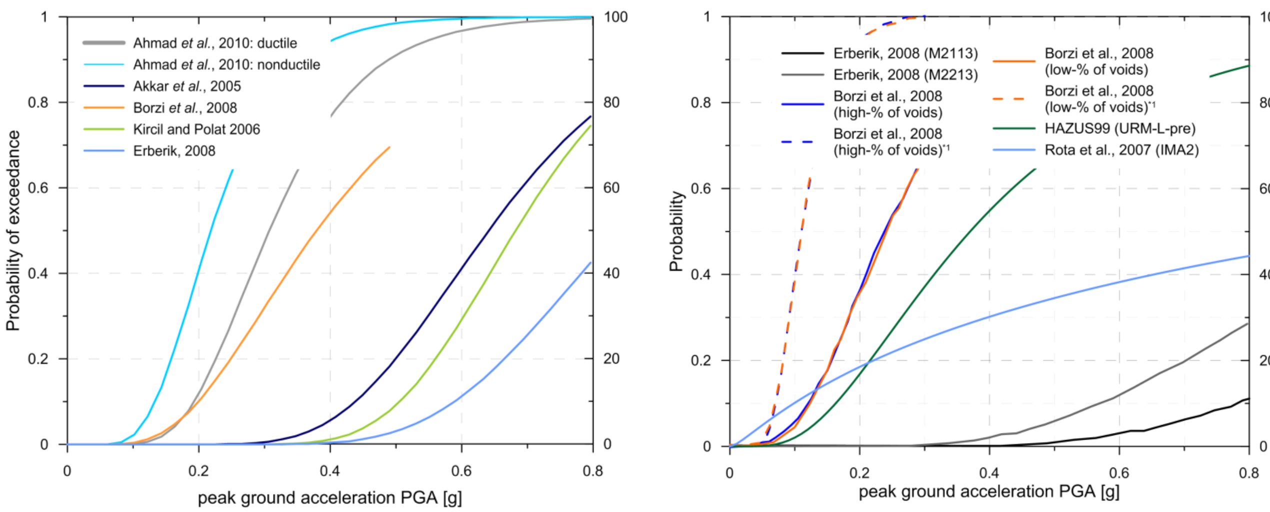

a) Five-story Reinforced Concrete (RC) structures b) Two-story brick masonry structures

*Figure 5. Comparison of available fragility functions proposed for RC and masonry building types for the limit state of collapse (including *1out-off-plane failure mechanism) (Abrahamczyk et al., 2016).*

Special studies on the basis of seismic building instrumentation

Similar for masonry and reinforced concrete building types a specific scheme of ranking criteria was used to identify representative buildings. Depending on the availability of the basic information describing the structural layout, buildings were selected for a multi-tasking in-situ instrumental testing procedure, which in each phase was related to the outcome of parallel analytical investigations by using different analysis methods and programmes. Temporarily installed weak-motion sensitive velocity-seismometers as well as permanent strong-motion building instrumentations could be used to measure the synchronous spatial building reaction at different elevations. On the basis of the instrumental data, the dynamic characteristics has been investigated and compared with the numerical results (Abrahamczyk et al., 2008; 2014). Figure 6 shows examples of instrumentally investigated buildings for Reinforced Concrete and masonry building types as well as observed damages caused by the 2023 Kahramanmaras, Turkey-Syria sequenced earthquake.

a) Masonry school building before and after the earthquake

b) RC frame structure

Figure 6. Examples of instrumented and investigated RC and masonry structures in part of the SERAMAR project before and after the 2023 Kahramanmaras earthquake.

Building-specific functions for residential RC buildings of Storey Class 2 (SC-2)

Within the SERAMAR project the concept of combination of low budget instrumental testing with analytical studies to carry out reliable and realistic damage prognosis for representative buildings of a specific building stock was introduced. Basic elements are the analytical assignment of the different damage grades on the basis of the material stress-strain-relationships and the numerical calibration of the structural models on the basis of the instrumentally gained dynamic response characteristics of the investigated building. After the determination of the relevant building response parameters the different damage grades can be allocated on the basis of the deformation states. Finally, fragility functions can be determined using the site-specific ground motion and representative earthquake records. (Abrahamczyk et al., 2014)

Figure 7a shows exemplarily the calibration results for a 5-story RC frame building by the modification of the stiffness of structural members (modifying the young's modulus), the distribution of the considered additional masses per story and by the adoption of the damping ratio of the structure. On the basis of the validated structural model the capacity curve and spectrum were determined and the different damage grades assigned according to (Schwarz et al., 2006). Finally, fragility functions for each damage grade and a set of strong motion records from Californian earthquakes (Schwarz et al, 2007) were derived (see Figure 7b).

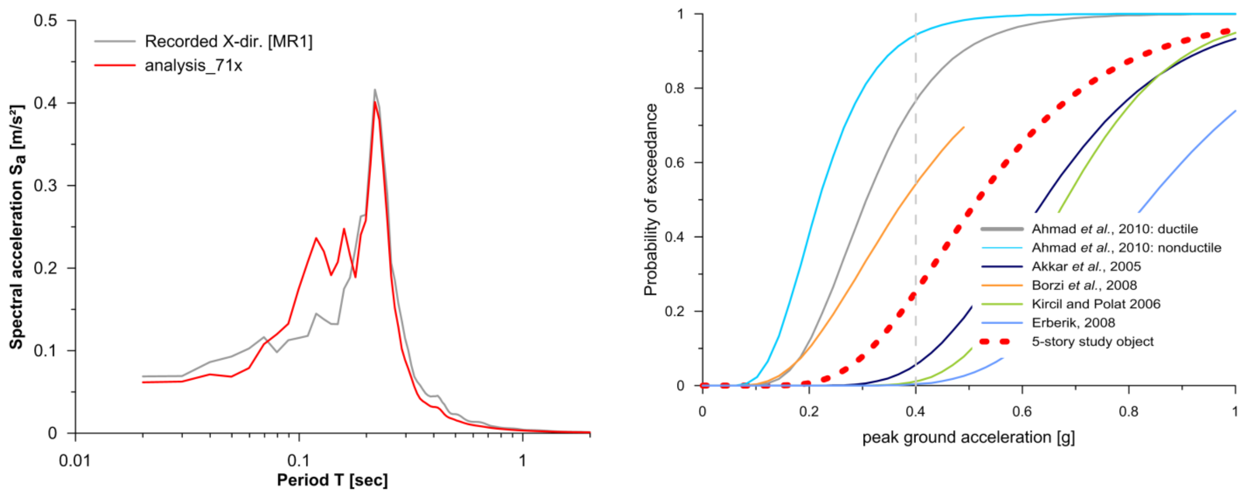

a) Response of calibrated model b) Fragility functions (collapse limit state)

Figure 7. Exemplarily calibration results and derived fragility functions by the use of low-budget building instrumentation data for 5-story RC frame structures with masonry infill walls.

4. Damage Scenarios

4.1 Previous results (Workshop 2010)

For a better comparison results of the damage probability of each damage grade were further used to determine the mean damage grade for each building type and the influence of the selected fragility functions on the results of the determined risk scenarios. For each set of fragility functions, the damage probability of each damage grade could be derived for the different building types (e.g. BT - basis type), for the different story classes and for the year of construction (see Figure 6). The application of the fragility functions according to (Ahmad et al., 2011) clearly show the different damage distributions depending on the story class and consideration of a ductile design for buildings constructed after 1999.

In Figure 8, the mean damage grades of empirical risk scenarios for Intensity *I (EMS) = IX* and a most likely vulnerability assignment are compared with the results of analytical risk scenarios for a (PGA) of 0.4g. Whereas the mean damage grade is the sum of the probability of each damage grade multiplied with a damage factor. The results indicate:

- the large scatter inherent to the different fragility functions for RC structures;
- the difficulties to select the fragility curves for an existing building stock;
- the huge differences between results from analytical and empirical approaches and
- the unclear and in some cases opposite trend between mean damage grade and story class.

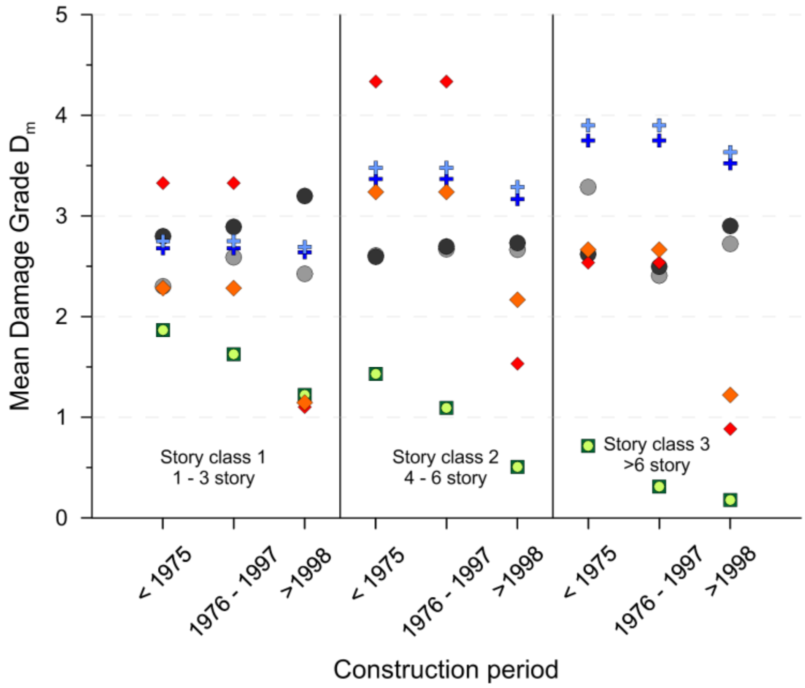

Figure 8. Comparison of the empirical (most likely) and analytical Mean Damage Grade for different story classes and construction years for Intensity I = IX and PGA value 0.4g.

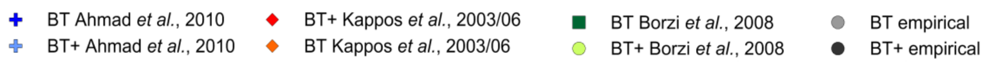

4.2. Results for 2023 Kahramanmaras earthquake sequence

Figure 9 shows the results for the seismic risk scenarios of intensities I_{Epi} = X and two variants of vulnerability assignments. Variant 1 (VC2) defines the vulnerability classes according to an optimistic ("most likely" assignment of vulnerability classes. Variant 2 (VC2) assumes a pessimistic distribution of the vulnerability classes, that is more probable based on the constructions and observed damages. In case of variant 2, the assigned vulnerability classes are downgraded by one class (e.g. B to A, C to B, etc).

For both variants, the methodology developed in Raschke (2004) is applied to determine structural damage in the form of damage degrees. In total 1000 Monte-Carlo simulations are carried out and mean-values as well as the 84% fractile of the damage grades determined. The epicentre is set on a fault north-east to Antakya (Reitmann, et al., 2023) and the site intensity determined for each individual building based on different intensity attenuation relationships (including the still quite valid by Sponheuer, 1960). Additionally, the site intensity is adjusted according to site conditions using the concept of with the delta intensities (Schwarz et al. 2005; 2006).

Within the next steps, the results will be compared with the observed (re-evaluated) damage grades – beginning with the assessment of the 2023 earthquake(s) by VHR satellite images while distinguishing between probably non-damaged, heavily destroyed and collapsed buildings (Hadidian & Schwarz, 2024).

5. Conclusions

In different phases of the Turkish–German joint research project on seismic risk assessment and mitigation in the Antakya-Maras region (SERAMAR), the seismic risk and the vulnerability of the building stock were determined based on the EMS-98 and a building stock survey. As it can be concluded from a series of comparative studies, models and vulnerability related functions of similar studies cannot be adopted directly. Because of their high vulnerability and the inherent heterogeneity due to the historical process of modifications and period-depending use of locally available material, it was decided to develop a new building typology, which should be supported by a complex evaluation and detailed investigation procedure.

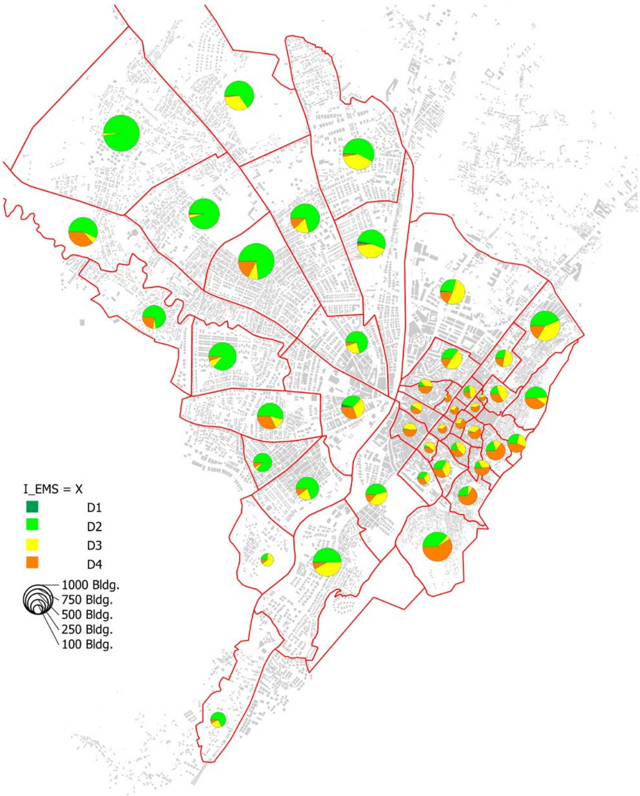

a) Intensity I_{EMS} = X (VC1), mean

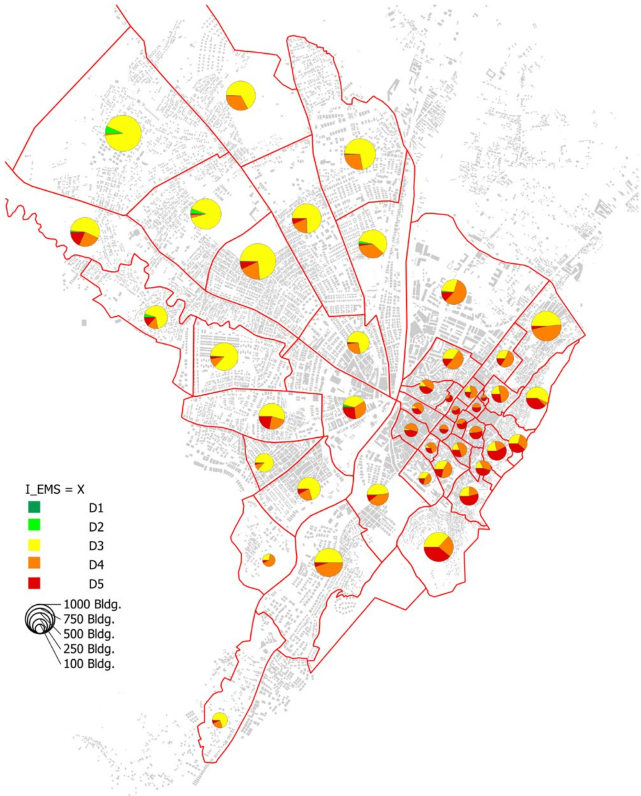

b) Intensity I_{EMS} = X (VC1), 84%-fractil

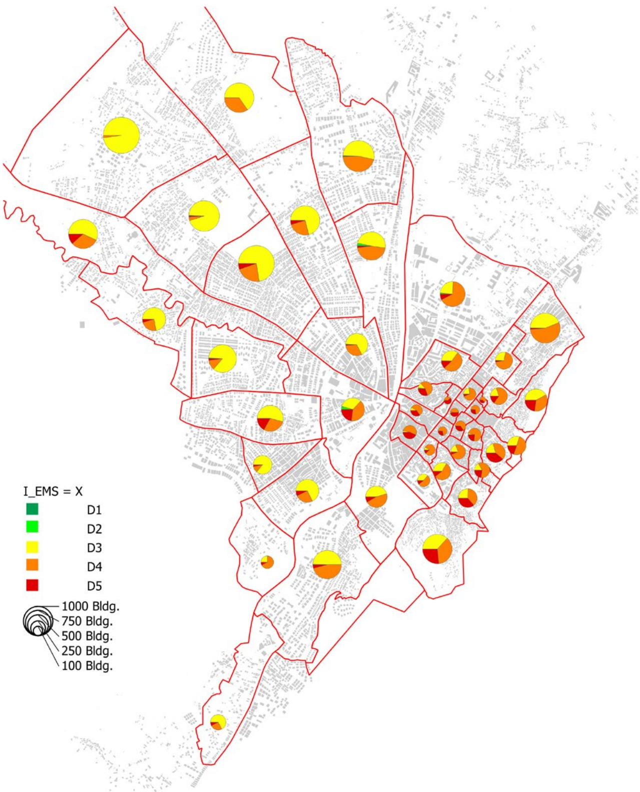

c) Intensity I_{EMS} = X (VC2), mean

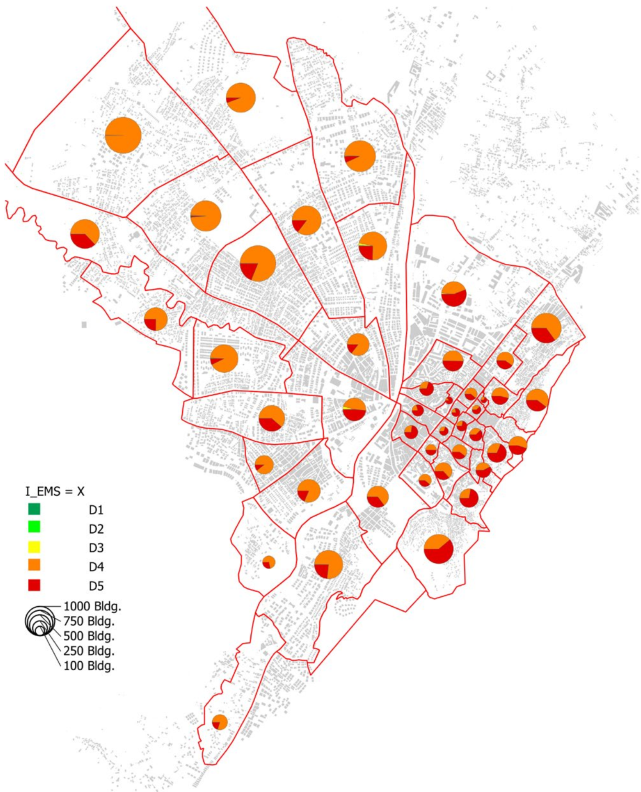

d) Intensity I_{EMS} = X (VC2), 84%-fractil

Figure 9. Distribution of Damage Grades (DG) for intensity I_{EMS} = X considering a most probable and pessimistic vulnerability assignment.

From the presented results, it can be concluded that the assignment of the vulnerability class has a strong influence on the damage prediction.

The results show the most vulnerable areas (hot spots) within the city Antakya and the general expectable loss (damage) in case of a strong event. In view of the recent event, the maps show the possible application within strategies to develop mitigation measures.

6. References

Abrahamczyk L., Schwarz J., Langhammer T., Genes M.C., Bikçe M., Kaçin S., Gülkan P. (2013). Seismic Risk Assessment and Mitigation in the Antakya–Maras Region (SERAMAR): Empirical Studies on the Basis of EMS-98. *Earthquake Spectra*, 29 (3), pp 683–704.

Abrahamczyk L., Schwarz J., Genes M.C. (2014). Qualification of seismic risk studies on the basis of instrumentally verified vulnerability functions for R.C. building types. In Proceedings: 10th U.S. National Conference on Earthquake Engineering, Anchorage Alaska, 21-25 July 2014.

AFAD Press Bulletin about the Earthquake in Kahramanmaraş—34 [EN/TR]—Türkiye | ReliefWeb. (2023, February 22). https://reliefweb.int/report/turkiye/afad-press-bulletin-about-earthquake-kahramanmaras-34-entr

Ahmad N., Crowley H., Pinho R. (2011). Analytical fragility functions for reinforced concrete and masonry buildings and building aggregates of Euro-Mediterranean regions. Department of Structural Mechanics, University of Pavia. WP3-Task 3.1 of SYNER-G under European Commission FP7 Project Technical report.

Erberik M.A., Yakut A., Genes M.C., Abrahamczyk L., Bikce M., Kacin S., Langhammer T., Gülkan P., Schwarz J. (2013). Characteristics of unreinforced masonry buildings in Antakya through filed survey. In Proceedings *2nd Turkish Conference on Earthquake Engineering and Seismology,* Antakya, Hatay/Turkey.

Grünthal G., Musson R., Schwarz J., and Stucchi M. (1998). European Macroseismic Scale 1998, Cahiers de Centre Européen de Géodynamique et de Seismologie, Volume 15, Luxembourg.

Hadidian M.N., Schwarz J. (2024). Damage Assessment of 2023 Earthquake by VHR satellite images implementing results of SERAMAR project. Proceedings of the *18th World Conference on Earthquake Engineering*, Milano, Italy.

Hancılar U., Şeşetyan K., Çaktı E., Şafak E., Yenihaya N., Malcıoğlu F.S., Dönmez K., Tetik T., & Süleyman H. (2023). Kahramanmaraş-Gaziantep Türkiye M7.7 Earthquake, 6 February 2023 (04:17 GMT+03:00) (No. V6). Boğaziçi University, Kandilli Observatory and Earthquake Research Institute Department of Earthquake Engineering.

Hasan P.L., Beinersdorf S., Schwarz J. (2023). Reliability of SHAKEmaps for rapid response decisions – as a question of time and generation procedure. *18. D-A-CH Tagung Erdbebeningenieurwesen & Baudynamik*, Sept. 14.-15., Kiel, Germany.

Kappos A.J., Panagiotopoulos C., Panagopoulos G., Papadopoulos E. (2003). WP4-reinforce concrete buildings (Level 1 and Level 2 analysis). RISK-UE Technical report.

Langhammer T., Schwarz J., Loukopoulus P., Abrahamczyk L., Karantoni F.V., Lang D.H. (2006). Intensity-based risk assessment for European Earthquake Regions – The 1995 Aigio Earthquake. *1st European Conference on Earthquake Engineering and Seismology (ECEES)*, Geneva, Switzerland.

Raschke M. (2004): Die Korrelation zwischen Erdbebenschaden und Erdbebenstärke und deren Anwendung in der Erdbebenrisikoanalyse. Dissertation, Bauhaus-Universität Weimar.

Reitman N.G., Briggs R.W., Barnhart W.D., Thompson Jobe J.A., DuRoss Ch.B., Hatem A.E., Gold R.D., Mejstrik J.D., and Akçiz S. (2023). Preliminary fault rupture mapping of the 2023 M7.8 and M7.5 Türkiye Earthquakes. DOI: https://doi.org/10.5066/P985I7U2

Schwarz J., Langhammer T., Kaufmann Ch. (2005). Quantifizierung der Schadenspotentiale infolge Erdbeben - Teil 1: Rekonstruktion des Bebens in der Schwäbischen Alb vom 03. September 1978. Bautechnik 82 (2005), Heft 8, 520-532. https://doi.org/10.1002/bate.200590170

Schwarz J., Langhammer T., Kaufmann Ch. (2006). Quantifizierung der Schadenspotentiale infolge Erdbeben Modellstudie Baden-Württemberg. Bautechnik 83 (2006) 12, 827-841 https://doi.org/10.1002/bate.200610072

Schwarz J., Abrahamczyk L., Leipold M., Swain T.M., Kaufmann Ch. (2006). Damage description for earthquake risk assessment. In Proceedings *1st European Conference on Earthquake Engineering and Seismology*, Geneva, Switzerland.

Schwarz J., Lang D., Kaufmann C., Ende C. (2007). Empirical ground-motion relations for Californian strong-motion data based on instrumental subsoil classification. *9th Canadian Conference on Earthquake Engineering*, Ottawa, Ontario, June 25-29, 2007.

Schwarz J., Langhammer T., Leipold M., Abrahamczyk L., Kaufmann Ch., Lang D.H., Riedel S. (2008). Bewertung der Erdbebenverletzbarkeit eines Gebäudestandes in innerstädtischen Großräumen – Phase 1 des SERAMAR Projektes. *Bauingenieur 83* – D-A-CH Mitteilungsblatt, 2–10

Schwarz J. (2010). Building typologies for empirical and analytical risk assessment: Case study Antakya, Presentation at Workshop on SERAMAR Project, 30 September 2010, Antakya, Turkey available at http://seramar.edac.biz/seramar1/html/Presentations%20all/session%201/Seramar_Schwarz_EDAC.pdf.

Schwarz J. (2011). Empirical vulnerability assessment – a review of contributions to the damage description for the European Macroseismic Scale, in Proceedings, *Earthquake Engineering and Engineering Seismology: Past Achievements and Future Prospects*, Ankara, Turkey.

Schwarz J., Abrahamczyk L., Leipold M., Wenk T. (2015). Vulnerability assessment and damage description for R.C. frame structures following the EMS-98 principles. *Bulletin of Earthquake Engineering*, 13(4), 1141-1159.

Schwarz J., Abrahamczyk L., Hadidian N., Haweyou M., Kaufmann Ch. (2021). Report on Knowledge-based exposure modelling framework depending on the accuracy and completeness of available data. Deliverable D4.1 TURNkey project H2020-SC5-2018.

Silva V., Crowley H., Colombi M. (2011). Fragility Function Manager Vers. 2.0. WP3 – Fragility Functions of Elements at Risk. Project No. 244061, Aristotle University of Thessaloniki, 2011.

Sponheuer W. (1960): Methoden zur Herdtiefenbestimmung in der Makroseismik. Veröffentlichungen des Instituts für Bodendynamik und Erdbebenforschung in Jena, 88, Berlin.

U.S. Geological Survey. (2023). M 7.8 - Pazarcik earthquake, Kahramanmaras earthquake sequence. Retrieved June 14, 2023, from https://earthquake.usgs.gov/earthquakes/eventpage/us6000jllz/executive

Wald D.J., Quitoriano V., Dengler L.A., & Dewey J.W. (1999). Utilization of the Internet for Rapid Community Intensity Maps. Seismological Research Letters, 70(6), 680–697. https://doi.org/10.1785/gssrl.70.6.680